Numerical Error in the k-ϵ Turbulence Model applied to Eddy-viscous Shock Waves

Krishnendu Sinha and Rachit S. Singh

Indian Institute of Technology Bombay, Mumbai, India 400076

1. Introduction

Interaction of shock waves with turbulent boundary layers often lead to high pressure and heat loads. Reynolds-averaged Navier Stokes (RANS) predictions are generally limited by the accuracy of turbulence models [1]. A large amount of research has focused on improving the physical modeling of turbulence amplification at shock waves. Shock waves are mathematical discontinuities in a flow, and are source of numerical error in a simulation. Large numerical error can result in physically unrealistic solution at shock waves [2] and the error may not decrease with successive grid refinement.

The majority of numerical methods employ numerical dissipation to capture a shock wave over two or three grid points. The RANS equations governing the mean flow are solved in a conservative form to limit the error at shock waves. In the k-ϵ equations, the production terms are usually not in conservative form, and can lead to large numerical error in a RANS simulation. Sinha and Balasridhar [2] proposed a transformation of variables to arrive at an alternate form of the k-ϵ equation, which eliminates the non-conservative production terms, without altering the physics. The new k-ϵ equations showed dramatic improvement in solution accuracy, especially for strong shock waves. The solution was found to be physically consistent and approached grid independence on successive grid refinement. Similar conservative method for the k-ω model was developed subsequently [3].

The previous results [2, 3] are based on inviscid analysis and simulations of the Euler equations at a shock wave. The effect of turbulent dissipation was retained, but the molecular and turbulent diffusion terms were neglected in the governing equations. This is representative of the limiting case with infinite Reynolds number, which is not the case in most practical applications. In addition, turbulent flows are highly dissipative, and the turbulent or eddy viscosity is often much larger than the molecular viscosity of the fluid. Turbulent diffusion results in an eddy-viscous shock wave, which is much thicker than a laminar shock. The effect of turbulent viscosity therefore must be included if the new k-ϵ model is to be applied to realistic flows.

It is interesting to note that the variable transformation proposed by Sinha and Balasridhar [2] makes the k-ϵ diffusion terms non-conservative. It is therefore important to examine the effect of possible non-conservative discretization error in the diffusion terms on the turbulence model predictions at a shock wave. This is the objective of the current note. We consider the interaction of homogeneous isotropic turbulence with a normal shock, which is also referred to as canonical shock-turbulence interaction in literature. The mean flow is one-dimensional and steady upstream and downstream of the shock wave, and it isolates the effect of the shock gradients on the turbulence, while eliminating additional complexities due to boundary layer gradients, flow separation and reattachment. The model problem has been studied extensively to gain physical insight and propose advanced RANS models for shock-dominated flows [4], [5].

2. Problem Formulation

We consider the k-ϵ model proposed by Sinha and Balashridhar [2] in terms of the transformed variables $f = k\rho^{-\frac{2}{3}c_0}$ and $g = \epsilon\rho^{-\frac{2}{3}c_1}$, where the parameters $c_0 = 1 - 0.4(1 - e^{(1-M_1)})$ and $c_1 = 1{+}0.21M_1$, are based on the shock-unsteadiness physics of Sinha et al. [4]. It has been shown that across a normal shock, $k \propto \rho^{\frac{2}{3}c_0}$ and $\epsilon \propto \rho^{\frac{2}{3}c_1}$ in the inviscid limit, and this forms the basis for the variable transformation. For canonical shock-turbulence interaction, the model equations can be written in one-dimensional form.

$$\rho u \frac{\partial f}{\partial x} = -\rho\epsilon\rho^{-\frac{2}{3}c_0} + \frac{\rho^{-\frac{2}{3}c_0}}{Re}\frac{\partial}{\partial x}\left[\left(\mu + \frac{\mu_t}{\sigma_k}\right)\frac{\partial k}{\partial x}\right], \tag{1}$$

$$\rho u \frac{\partial g}{\partial x} = -c_2\frac{\rho\epsilon^2}{k}\rho^{-\frac{2}{3}c_1} + \frac{\rho^{-\frac{2}{3}c_1}}{Re}\frac{\partial}{\partial x}\left[\left(\mu + \frac{\mu_t}{\sigma_\epsilon}\right)\frac{\partial \epsilon}{\partial x}\right], \tag{2}$$

where ρ and μ are Reynolds-averaged quantities, u is Favre-averaged velocity and $\mu_t = c_\mu\rho k^2/\epsilon$ is the turbulent eddy viscosity. The model constants are $c_\mu = 0.09$, $c_2 = 1.92$, $\sigma_k = 1.0$ and $\sigma_\epsilon = 1.3$. The left-hand side represents the convection of the transformed turbulence variables, and the terms on right-hand side represent the dissipation and diffusion effects. Note that the non-conservative production terms are not explicitly present in the equations, but their physical effects are included in the definition of new turbulence variables f and g. The above equations are in non-dimensional form, where the mean speed of sound a_1^*, mean density ρ_1^* and mean viscosity μ_1^* in the upstream flow are taken as the characteristic quantities. The most energetic wave number κ_0 in the incoming turbulence field is used to define the characteristic length scale. The turbulent kinetic energy k and its dissipation rate ϵ are thus non-dimensionalized by a_1^{*2}

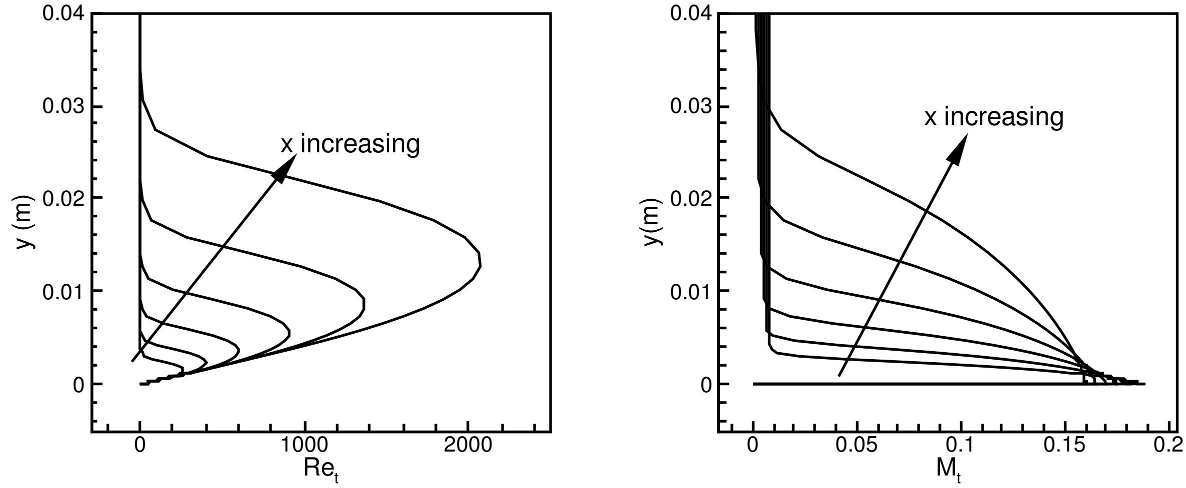

(a) (b)

Figure 1: Turbulent Reynolds number and turbulent Mach number are plotted as a function of the wall-normal distance for a Mach 2.84 boundary layer at x-locations (in m) of 0.15, 0.58, 1.03, 1.51, 2.02 and 2.55 along a flat plate.

and $a_1^{*3}\kappa_0$, respectively, where the $*$ represents the dimensional quantities and subscript 1 denotes shock-upstream values.

The diffusion terms are active in the high-gradient region of the shock wave and it smooths out the large variations in the flow variables. They are expected to reduce the amplification in turbulence quantities at the shock. The diffusion term in (1) can be expanded as

$$\begin{aligned} &\frac{\rho^{-\frac{2}{3}c_0}}{Re}\frac{\partial}{\partial x}\left[\mu\left(1+\frac{Re_t}{\sigma_k}\right)\frac{\partial k}{\partial x}\right] \\ \simeq\quad &\rho^{-\frac{2}{3}c_0}\left[\mu\frac{Re_t}{Re}\frac{\partial^2 k}{\partial x^2}+\frac{Re_t}{Re}\frac{\partial\mu}{\partial x}\frac{\partial k}{\partial x}+\frac{\mu}{Re}\frac{\partial Re_t}{\partial x}\frac{\partial k}{\partial x}+\ldots\right], \end{aligned} \tag{3}$$

where we assume $Re_t = \mu_t/\mu \gg 1$ for realistic flows (see Table 1). A similar expansion can be written for the diffusion term in (2), where $\sigma_\epsilon \simeq 1$. The viscous and turbulent diffusion effects depend on Re, Re_t and the gradients of μ, k and ϵ at the shock. The gradients in the mean flow and turbulence quantities depend on the shock thickness δ and their jump across the shock wave. The shock jumps are determined solely by the upstream Mach number M_1 and the ratio of specific heats γ (taken to be 1.4 in this work). The shock thickness is generally determined by the numerical dissipation of the method and grid resolution.

The physical parameters governing the effect of diffusion are M_1, Re and Re_t. Larsson and Lele [6] present DNS of canonical shock-turbulence interaction for a series of Mach numbers. The turbulent Mach number is 0.22 and the Reynolds number based on Taylor micro-scale is 40. These values are used to compute the normalized values of k and ϵ upstream of the shock

$$k_1 = \frac{1}{2}M_t^2 = 0.0242 \quad \text{and} \quad \epsilon_1 = \frac{5}{\sqrt{3}}\frac{1}{\kappa_0\lambda^\star}\frac{M_t^3}{Re_\lambda} = 9.1\times10^{-4}, \tag{4}$$

where the pre-shock Taylor length scale is $\kappa_0\lambda^\star = 0.842$. The Reynolds numbers are further computed as

$$Re = \frac{\sqrt{3}}{k_o\lambda^\star}\frac{1}{M_t}Re_\lambda = 374 \quad \text{and} \quad Re_t = c_\mu\frac{\rho k^2}{\epsilon\mu}Re = 21.6\,,$$

where the mean and turbulent flow quantities are in non-dimensional form. The DNSs [6] are limited to low values of Reynolds number and the flows with $M_1 = 1.5$, 2.5, 3.5 and 4.7 are used as test cases in the present study. Additional cases at intermediate Mach numbers are also computed using the parameter values listed above.

To study practically relevant range of Reynolds numbers, we consider a representative turbulent boundary layer on a flat plate. The free-stream Mach number is taken as 2.84 corresponding to Settles 24° compression ramp experiment [7]. RANS solution is computed using a low Reynolds number k-ϵ turbulence model, and the numerical method is identical to that presented in [5]. Fig. 1 shows the variation of Re_t and M_t at different streamwise locations along the plate. The peak value of Re_t along with the values of M and M_t at each location are listed in Table 1. In the absence of peak-energy wave number for these cases, the boundary layer thickness is taken as the characteristic length scale, and the corresponding Reynolds numbers are included in the table. These are used to set up equivalent canonical STI cases to isolate the effect of turbulent diffusion at realistic flow conditions.

3. Error Analysis

The convection terms in (1) and (2) can be written in conservative form using the mass conservation equation across the shock wave [2]. The discretization error in the convective terms therefore vanish as the grid is refined. The dissipation term

Table 1: Flow parameters from RANS solution of flat-plate boundary layer at different locations (in m) downstream of the plate tip.

M	M_t	Re	Re_t	Re_t/Re	location
2.338	0.143	5.39E+04	1.89E+02	3.50E-03	0.15
2.384	0.129	1.64E+05	6.26E+02	3.81E-03	0.58
2.412	0.123	2.59E+05	1.03E+03	2.83E-03	1.03
2.421	0.120	3.52E+05	1.43E+03	4.06E-03	1.51
2.434	0.117	4.42E+05	1.82E+03	4.12E-03	2.02
2.437	0.116	5.35E+05	2.16E+03	4.04E-03	2.55

does not include derivative of flow variables, and is therefore well-behaved in the high-gradient region of a shock wave. By comparison, the diffusion terms are non-conservative in nature and can potentially lead to large error at flow discontinuities. In the finite-volume formulation, they are discretized in terms of fluxes computed at the cell faces $i \pm 1/2$

$$\frac{1}{Re}\rho^{-\frac{2}{3}c_0}\left(\frac{h_{i+1/2}-h_{i-1/2}}{\Delta x}\right), \quad \text{where} \quad h=\left(\mu+\frac{\mu_t}{\sigma_k}\right)\frac{\partial k}{\partial x} \tag{5}$$

and Δx is the cell size. Taylor series expansion leads to

$$\frac{1}{Re}\rho^{-\frac{2}{3}c_0}\left[\left(\frac{\partial h}{\partial x}\right)_i+\frac{\Delta x^2}{24}\left(\frac{\partial^3 h}{\partial x^3}\right)_i+O(\Delta x^4)\right], \tag{6}$$

where the second term is the leading order truncation error. Consider only the first term in the series and integration by parts leads to,

$$\begin{aligned} &\frac{1}{Re}\int_{i-\frac{1}{2}}^{i+\frac{1}{2}}\rho^{-\frac{2}{3}c_0}\frac{\partial h}{\partial x}dx \\ &= \frac{1}{Re}\left[\rho^{-\frac{2}{3}c_0}h\right]_{i-\frac{1}{2}}^{i+\frac{1}{2}}-\frac{1}{Re}\int_{i-\frac{1}{2}}^{i+\frac{1}{2}}-\frac{2}{3}c_0\rho^{-(\frac{2}{3}c_0+1)}\frac{\partial\rho}{\partial x}hdx \end{aligned} \tag{7}$$

The integrated effect across the entire shock is thus given by,

$$\frac{1}{Re}\left[\rho^{-\frac{2}{3}c_0}\left(\mu+\frac{\mu_t}{\sigma_k}\right)\frac{\partial k}{\partial x}\right]_{up}^{dn}+\frac{2}{3}\frac{c_0}{Re}\int_{up}^{dn}\rho^{-(\frac{2}{3}c_0+1)}\frac{\partial\rho}{\partial x}\left(\mu+\frac{\mu_t}{\sigma_k}\right)\frac{\partial k}{\partial x}dx. \tag{8}$$

The first term is conservative and its contribution across the shock is small, because of negligible k-gradient at the upstream (up) and downstream (dn) edges of the shock wave. The second term is non-conservative and can be written as

$$\frac{4}{9}\frac{c_0^2}{Re}\int_{up}^{dn} f\left(\frac{1}{\rho}\frac{\partial\rho}{\partial x}\right)^2\left(\mu+\frac{\mu_t}{\sigma_k}\right)dx \tag{9}$$

by assuming that $f = k\rho^{-\frac{2}{3}c_0}$ is constant across the shock. This is true for inviscid shock waves [4], and is approximately valid for eddy-viscous shock waves, as per the simulation results presented in the next section.

Now, we estimate the magnitude of the different terms as

$$\left(\frac{1}{\rho}\frac{\partial\rho}{\partial x}\right)^2 \simeq \left[\frac{1}{\rho_{av}}\frac{2(\rho_{av}-1)}{\delta}\right]^2 \sim \frac{1}{\delta^2} \tag{10}$$

where ρ_{av} is the average density across the shock and the upstream density is normalized to 1. Also, for highly turbulent flows $\mu+\mu_t/\sigma_k \sim \mu Re_t$, where the fluid viscosity $\mu \propto T^{0.75} \sim M^{1.5}$, as the temperature jump across a normal shock scales as M^2 for high Mach numbers. For normalized $f \simeq 1$ across a shock, we have

$$\frac{4}{9}\frac{c_0^2}{Re}\int_{up}^{dn} f\left(\frac{1}{\rho}\frac{\partial\rho}{\partial x}\right)^2\left(\mu+\frac{\mu_t}{\sigma_k}\right)dx \quad \sim \quad \frac{1}{\delta}\frac{Re_t}{Re}M^{1.5} \tag{11}$$

The non-conservative part of the diffusion term (7) is proportional to Re_t, and hence its effect is larger at higher turbulence levels. The effect is inversely proportional to the Reynolds number of the flow and the shock thickness. Its magnitude is higher for stronger shock waves with higher downstream value of the dynamic viscosity μ.

As per (11), the non-conservative contribution of the diffusion terms scale as Re_t/Re; typical values of this ratio are 10^{-2} or lower for realistic flows (see table 1). Its effect is expected to increase with grid refinement, as δ decreases. For fine enough grids, the shock thickness is determined by the balance of the diffusion terms and the inertial terms in the governing equations. An equivalent Reynolds number defined in terms of the shock thickness and the sum of molecular and turbulent viscosity is therefore order 1 in magnitude. This can be used to show that the shock thickness scales as $\delta \sim Re_t/Re$ for very fine mesh. Thus, the overall non-conservative effect of the diffusion terms, given by (11), is bounded for finite Mach numbers, and a well-behaved solution is expected in the limit of $\Delta x \to 0$.

A similar analysis of the truncation error in (6) leads to an integrated effect across the shock

$$\begin{aligned} &\frac{\Delta x^2}{24}\frac{1}{Re}\int_{up}^{dn}\rho^{-\frac{2}{3}c_0}\frac{\partial^3}{\partial x^3}\left[\left(\mu+\frac{\mu_t}{\sigma_k}\right)\frac{\partial k}{\partial x}\right]dx \\ &\sim \frac{1}{Re}\frac{\Delta x^2}{24}\rho_{av}^{-\frac{2}{3}c_0}\mu_{av}Re_t\frac{[k]}{\delta^4}\int_{up}^{dn}dx \\ &\sim \frac{\Delta x^2}{24}\frac{Re_t}{Re}M^{1.5}\frac{1}{\delta^3}, \end{aligned} \tag{12}$$

where the jump $[k]$ across the shock is taken to be order 1 in magnitude (supported by the simulation results presented in the next section), and the average viscosity μ_{av} is assumed to scale as $M^{1.5}$, as earlier. For shock capturing schemes, $\Delta x \propto \delta$ and therefore the above scaling of the truncation error is comparable to the estimate of the non-conservative diffusion term in (11),

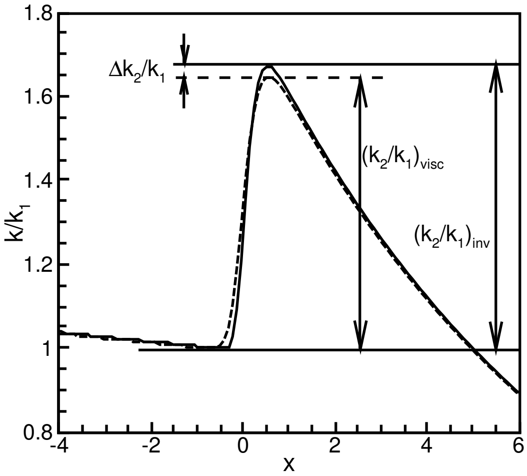

Figure 2: Jump in turbulent kinetic energy across a Mach 3.5 normal shock obtained from inviscid (solid) and viscous (dashed) simulations show the effect of diffusion at the shock wave.

possibly lower by a factor of 1/24. The magnitude of both (11) and (12) are small compared to convection and production at the shock for realistic combinations of Re and Re_t. The foregoing analysis indicates that the error is also bounded in the limit of infinitely fine grid, and the same can be shown for the ϵ-diffusion term.

4. Simulation results

The one-dimensional Reynolds-averaged Navier-Stokes equations are solved for the mean flow, with (1) and (2) used for turbulence closure. The non-dimensionalization is as described in section II. The equations are integrated using the conservation form of Lax-Friedrichs scheme. The code had been successfully used to reproduce results from [2], which were obtained using Steger-Warming flux-vector splitting method. The Lax-Friedrichs scheme requires more number of grid points to obtain identical results for a particular Mach number, when compared with the code used in [2]. The diffusion terms are solved with second-order central difference scheme, and explicit time integration is achieved using the first-order forward Euler method. The computational domain ranges from $x = -7.6$ to 29.6, and the initial and boundary conditions are as described in [2]. The solution is obtained on 400 equispaced grid points and the effect of grid refinement is discussed subsequently.

Figure 2 plots the stream-wise variation of turbulent kinetic energy in a canonical shock-turbulence interaction. Results obtained using inviscid and viscous simulations are compared, and the region near the shock wave, located at $x = 0$, is magnified. As expected, the viscous simulation results in a slightly thicker shock, and a slightly lower amplification in k and ϵ (not shown), compared to the inviscid case. The data is normalized by the TKE immediately upstream of the shock, given by (4), such that the peak values correspond to the respective amplification factors. The difference between the inviscid and viscous k_2/k_1 is denoted by $\Delta k_2/k_1$, and is used to quantify the effect of viscous and turbulent diffusion at the shock wave.

The inviscid and viscous amplification factors for TKE and its dissipation rate are plotted for a range of Mach numbers in Fig. 3. The results are compared with the inviscid results obtained using the modified Steger-Warming method [2], and the exact inviscid solution is presented for reference. The amplification of TKE increases with Mach number to reach an asymptotic value in the hypersonic limit, while the amplification in ϵ increases monotonically with shock strength. All curves follow the same trend as the respective inviscid exact solutions, but are different in magnitude, due to the varying degree of diffusion effects. Comparison of the inviscid results obtained by the two numerical methods bring out the effect of numerical viscosity. A dissipative scheme, like the Lax-Friedrich method, results in a significantly lower TKE amplification than the low-dissipation (modified) Steger-Warming method. Additional effects of molecular and turbulent diffusion in the Lax-Friedrich viscous solution results in further lowering of the TKE and ϵ jumps across the shock.

The effect of viscous and turbulent diffusion on turbulence amplification for varying Reynolds and Mach numbers is shown in Fig. 4. The quantities $\Delta k_2/k_1$ and $\Delta\epsilon_2/\epsilon_1$, as shown in Fig. 2, are plotted against the ratio of the turbulent Reynolds number and the characteristic Reynolds number of the flow. The entire range of Reynolds numbers ($5.39 \times 10^4 - 5.35 \times 10^5$) and turbulent Reynolds number ($1.89 \times 10^2 - 2.16 \times 10^3$), listed in Table 1, are plotted, and we use a log scale to span the parameter space. All the data for a fixed Mach number collapse into a single line, and the different Mach number lines are offset by a fixed amount independent of the ratio Re_t/Re (clearly seen in the ϵ-plot in Fig. 4). The results indicate a power-law variation with Re_t/Re, as expected from the error analysis presented in the previous section. For a fixed Re_t/Re, the TKE data appears to saturate for high Mach numbers, as expected from Fig. 3. The viscous effect on ϵ, on the other hand, shows monotonic increase with increasing Mach number. This is possibly because of the higher magnitudes of ϵ-amplification and a consequent higher effect of eddy viscosity on a higher peak ϵ, as compared to TKE jump across the shock wave. Overall, the jump in the turbulence quantities across an eddy-viscous shock wave is very close to those in an inviscid computation. The effect on the normalized k and ϵ are in the range of 10% or lower for practically relevant range of Mach and Reynolds numbers.

The k-ϵ solutions computed on successively refined grids with 200, 400, 800 and 1200 equi-spaced points (cell sizes of 0.186, 0.093, 0.047 and 0.031 respectively) are shown in Fig. 5. As expected, a finer mesh gives a finer shock and higher jumps in k and ϵ across the shock wave; there is very little change in the solution on either side of the shock. The results show a systematic convergence to a grid-independent solution. The results are also fairly close to the DNS data, except for the high TKE values obtained in the unsteady shock region, which represent shock oscillations [6]. The effect of grid refinement on the peak k and ϵ are plotted as a function of Re_t/Re in Fig. 6. The data

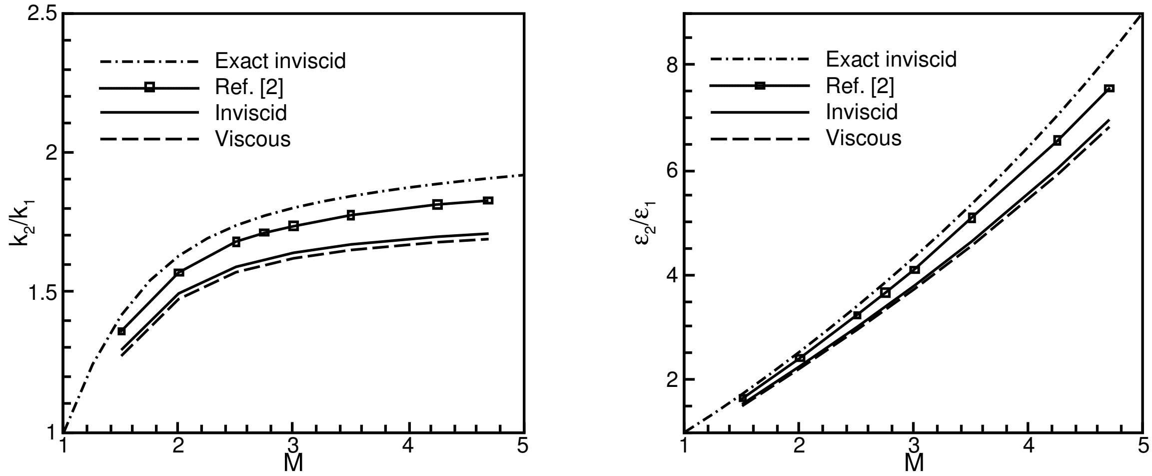

(a) (b)

Figure 3: Peak TKE and ϵ obtained using the modified Steger-Warming method (reproduced from Ref. [2]) and the inviscid/viscous simulations using the Lax-Friedrich method for a range of Mach numbers.

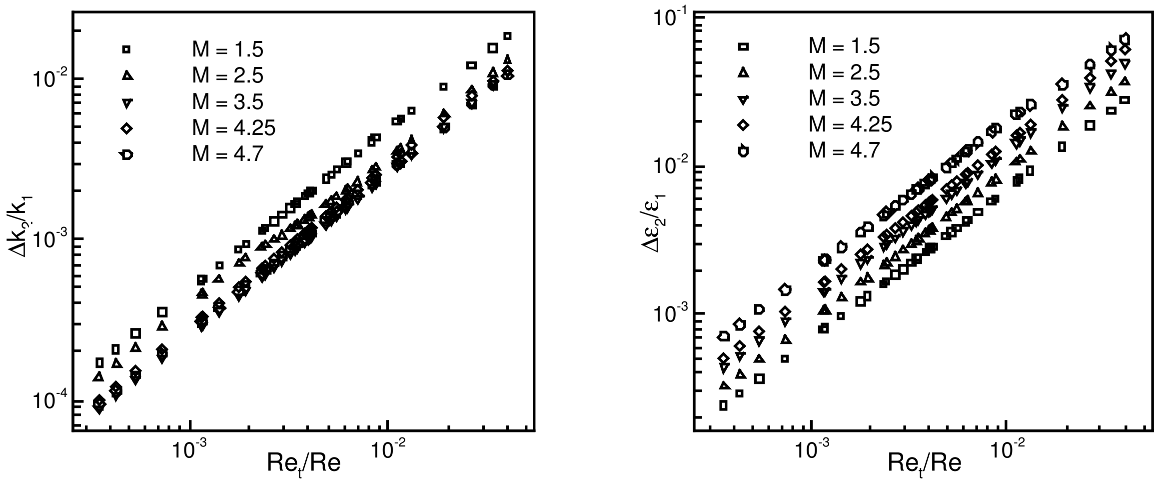

(a) (b)

Figure 4: Effect of turbulent diffusion on the shock-amplification in TKE and ϵ at varying Reynolds numbers, for different Mach numbers.

shows an identical trend as in Fig. 4, with the finer grid results placed higher for all Reynolds numbers. The data also shows a converging trend with grid refinement, especially for the turbulent dissipation rate. We thus obtain well-behaved solution in the limit of infinitely fine computational mesh, and the effect of non-conservative diffusion terms in the k-ϵ equations is bounded.

We note that the effect of the viscous/turbulent diffusion and the corresponding errors are small in magnitude for the k-ϵ model proposed by Sinha and Balasridhar [2]. This may not be the case for other turbulence models, which predict very high amplification in k and ϵ at the shock. Examples include the standard k-ϵ model and the shock-unsteadiness k-ϵ model [4] with non-conservative production terms. We see a large effect of the turbulent diffusion terms in the shock-unsteadiness k-ϵ model, where the amplification in ϵ can vary by upto 40% between the inviscid and the viscous simulations for a given Mach number and grid resolution. This is because of the fact that the normalized ϵ is much larger than 1, unlike what is assumed in the analysis presented in section III. A suitable modification can be introduced to estimated the diffusion effects for such models.

5. Conclusion

This note presents error analysis of the non-conservative diffusion terms in a k-ϵ model that has been previously shown to be numerically robust for inviscid shock waves. The error in

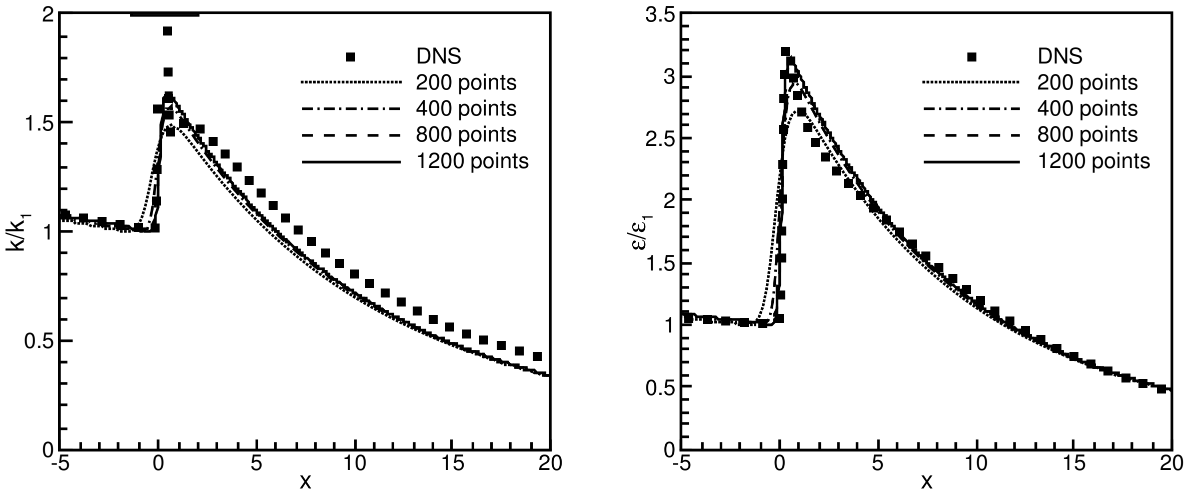

(a) (b)

Figure 5: Evolution of TKE and its dissipation rate in a Mach 2.5 canonical shock turbulence interaction computed on successively refined grids, and compared to DNS [6].

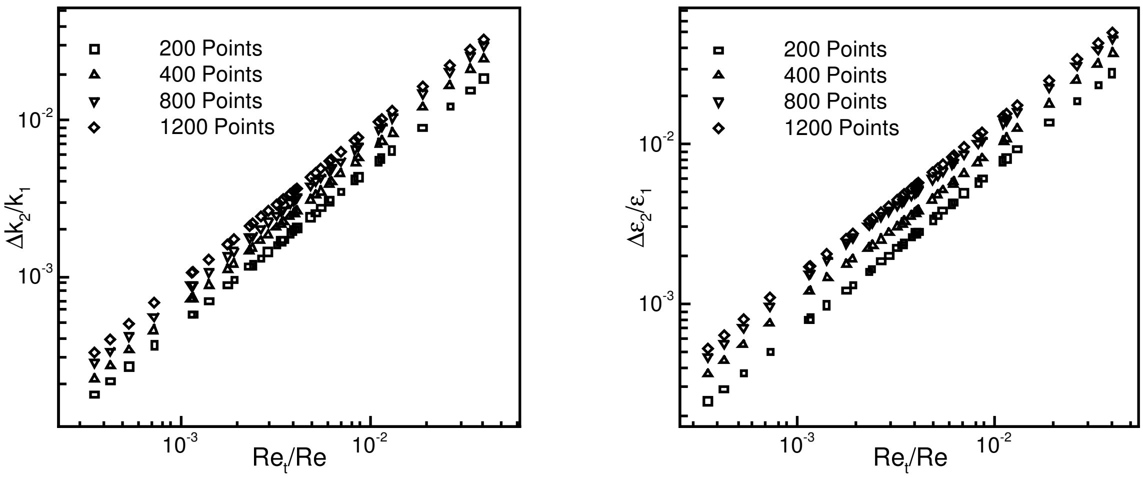

(a) (b)

Figure 6: Grid convergence of the turbulent diffusion effect on TKE- and ϵ-amplification at varying Reynolds numbers, for Mach number of 1.5.

eddy-viscous shocks is found to scale with the ratio of the turbulent Reynolds number and the characteristic Reynolds number of the flow. It also increases with shock Mach number and for a thinner shock wave computed on a finer mesh. Numerical simulations presented for a range of parameters substantiate the error estimate, and show that the effect of non-conservative derivatives in the diffusion terms is minimal for realistic values of Reynolds number. The error remains bounded and small on successive grid refinement, and the model equations accurately reproduce DNS data of shock-turbulence interaction. The current k-ϵ model is thus shown to be numerically robust at shock waves with eddy-viscous effects.

References

[1] C. J. Roy, F. G. Blottner, Review and assessment of turbulence models for hypersonic flows, Progress in Aerospace Sciences 42 (7) (2001) 469–530.

[2] K. Sinha, S. J. Balasridhar, Conservative Formulation of the k-ϵ Turbulence Model for Shock-Turbulence Interaction, AIAA Journal Vol. 51, No. 8, (2013) 1872–1882, doi:10.2514/1.J052289.

[3] K. Sinha, S. J. Balasridhar, A Conservative k-ω Model for Shock Dominated Flows, The 5th European Conference for Aeronautics and Space Sciences, Munich, Germany .

[4] M. K. Sinha, K., G. V. Candler, Modeling Shock-Unsteadiness in Shock/Turbulence Interaction, Physics of Fluids Vol. 15, No. 8, (2003) 2290–2297, doi:10.1063/1.1588306.

[5] M. K. Sinha, K., G. V. Candler, Modeling the Effect of Shock-Unsteadiness in Shock/Turbulent Boundary-Layer Interactions, AIAA Journal Vol. 43, No. 3, (2005) 586–594, doi:10.2514/1.8611.

[6] J. Larsson, S. K. Lele, Direct Numerical Simulation of Canonical Shock/Turbulence Interaction, Physics of Fluids Vol. 21, No. 12, (2009) 126101, doi:10.1063/1.3275856.

[7] F. T. J. Settles, G. S., S. M. Bogdonoff, Detailed Study of Attached and Separated Compression Corner Flowfields in High Reynolds Number Supersonic Flow, AIAA Journal 17(6).